Int. Agrophysics, 1994, 8, 393-402

USING THE HELMHOLTZ INTEGRAL TO PREDICT THE ACOUSTIC RADIATION FROM A VIBRATING APPLE DURING NON-CONTACT FREQUENCY RESPONSE MEASUREMENTS

H. Chen, J. De Baerdemaeker

Department of Agricultural Engineering, Katholieke Universiteit Leuven, Kardinaal Mercierlaan 92, 3001 Heverlee, Belgium

A b s t r a c t. Helmholtz integral is used to predict the acoustic pressure radiation near a vibrating apple. Solution approaches are developed for the acoustic pressure of the spherical mode of an apple with a revolutionary shape. The distribution of the surface pressure as well as the pressure radiation from the apple surface are obtained. The influence of the apple properties and the transmission medium property on the distribution and magnitude of the pressure is analysed.

K e y w o r d s: apple, acoustic radiation, pressure radiation

INTRODUCTION

Fruit firmness could be evaluated in nondestructive way by means of the resonant frequency obtained from the transfer function or response spectrum of the intact fruit. In the earlier measurement systems, the accelerometer was normally used as a sensor for the response signal. During measurement, the accelerometer was attached to the fruit by using elastic band, flexible film or clay [9,10,14]. Such an attachment is time consuming, and makes automatic measurement much more difficult to be realised. Furthermore, it may cause more damage to the apple. To have this nondestructive technique commercially available, the measurement system was improved these years by replacing the accelerometer with the microphone as response sensor [1,3,12,15]. This improvement makes the attachment of a response sensor on the fruit surface unnecessary. With the microphone, the signal measured is the pressure radiated from the fruit surface through a certain distance in the air. In this paper, Helmholtz integral is attempted to predict the pressure radiation from the apple surface. The objective of this effort is to establish a theoretical means and solution approaches for a better understanding of the signal measurement with the microphone. This can possibly guide a proper design of the measurement set-up.

GOVERNING EQUATIONS

To simulate the vibration of an intact fruit, Navier's equation for the small motion of a homogeneous, isotropic, elastic body is used [1,7,12]:

$$(\mu + \lambda)\,(\nabla \cdot u) + \mu\, \nabla^2 u = \rho \ddot{u} \qquad (1)$$

where μ,l are Lamé constants, u is the displacement vector, ρ is the density of the body. In case of spherical vibration, u can be defined by a scalar potential Φ [2]:

$$u = \varphi \qquad (2)$$

which upon being substituted into Eq. 1 yields the elastic wave equation [1,7]:

$$\frac{\partial^2 \Phi}{\partial t^2} = c^2\, \nabla^2\, \Phi \qquad (3)$$

where c is the velocity of sound in the body. According to Euler's equation for the conservation of momentum [11], the acoustic pressure P at an arbitrary point in the body is obtained as:

$$P = -\rho \frac{\partial^2 \Phi}{\partial t^2} \tag{4}$$

When the body is subjected to a sinusoidal vibration, Φ can be separated into two functions [2]:

$$\Phi(r,t) = \varphi(r)\, e^{i\omega t} \tag{5}$$

where r is the distance between a field point and a source point, ω is the radian frequency. Substituting Eq. 5 into Eq. 4, we have the simplified form of P as:

$$P(r,t) = \rho\, \omega^2 \varphi(r)\, e^{i\omega t} = p(r)\, e^{i\omega t} \tag{6}$$

where

$$p(r) = \rho\, \omega^2 \varphi(r) \tag{7}$$

Substituting Eqs 5 and 6 into Eq. 3 results in the Helmholtz equation for the acoustic pressure:

$$\nabla^2 p + k^2 p = 0 \tag{8}$$

where

$$k = \frac{\omega}{c} \tag{9}$$

Applying Green's theorem to Eq. 8 gives the Helmholtz integral for the external field problems [2,8]:

$$p(T) = -\frac{1}{2\pi} {}^{x}\!\int\!\!\int \left[G(T,Q)\, \frac{\partial p(Q)}{\partial n_Q} - p(Q)\, \frac{\partial G(T,Q)}{\partial n_Q} \right] dA \tag{10}$$

and

$$p(R) = -\frac{1}{4\pi} \int\!\!\int \left[G(R,Q)\, \frac{\partial p(Q)}{\partial n_Q} - p(Q)\, \frac{\partial G(R,Q)}{\partial n_Q} \right] dA \tag{11}$$

where Q and T are two field points on the vibrating surface A, R is an external field point, and n_Q is the outward unit vector normal to the surface at point Q, as shown in Fig. 1. The starred integral sign denotes

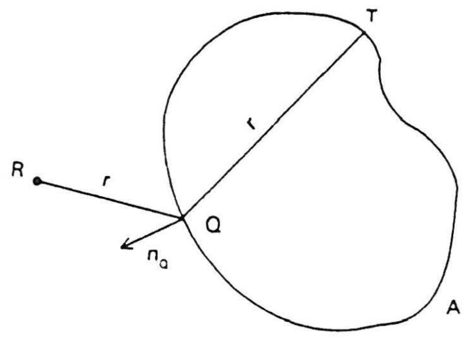

Fig. 1. Helmholtz integral for the general problem.

that the principal value of the improper integral is to be taken. G is the Green's function defined by:

$$G(T,Q)\, \frac{e^{ikr}}{r} \tag{12}$$

It is important to note that Eqs 10 and 11 only involve pressure integration over the vibration surface of the elastic body. Eq. 10 should first be solved for the surface acoustic pressure, and these values are then substituted into Eq. 11 for the acoustic pressure at an external field point R.

The pressure gradient on the boundary surface in Eqs 10 and 11 is usually defined by the boundary condition [6,8]:

$$\frac{\partial p}{\partial n} = i\, \rho\, \omega\, v_n \tag{13}$$

where $i = \sqrt{-1}$. When the distribution of the normal velocity v_n of a spherical mode on the vibration surface is available, i.e. Eq. 13 is given, the pressure distribution can be obtained by directly solving Eq. 10.

SOLUTION APPROACHES

In the above, the general integral equations for arbitrary surface shape were introduced along with a boundary condition to fully describe the external acoustic pressure. In view of the characteristics of the apple shape and its spherical mode [5], the integral equations and the boundary condition can first be simplified, and then solved by numerical approaches.

Simplification of the general acoustic problem

The apple shape can be regarded as a y-axisymmetric revolution. For such kind of boundary surface, Chertock [6] gives a fairly general class of vibration velocity distributions:

$$v\,(x,y,\theta) = v(x,y)\cos(m\,\theta) \qquad (14)$$

where x, y, and θ are the cylindrical coordinates of any point on the apple surface. For the spherical mode, m equals 0. This means that the vibrational velocity in the circle around y axis on the apple surface is constant. The boundary condition Eq. 13 hence becomes:

$$\frac{\partial p}{\partial n} = i\,\rho\,\omega\,v\,(x,y) \qquad (15)$$

This boundary condition is now simplified from a three dimensional problem to a two dimensional problem. Substituting Eqs 12 and 15 into Eq. 10 yields:

$$p\,(T) = -i\int_{\Gamma} V(Q)\,T(T,Q)\,ds + \int_{\Gamma} P\,(Q)\,U(T,Q)\,ds \qquad (16)$$

where $V(Q)$, $T(T,Q)$ and $U(T,Q)$ are listed in the appendix, s is the segmental arc in the boundary line on x-y plane, Q and T turn out to be the points on this line. Equation 10 is now transformed to the two-dimensional integral equation along the boundary line Γ. If we designate the real and the imaginary parts by the superscripts r and i, e.g., $p\,(T)=p^{r}(T)+i\,p^{i}(T)$, then Eq. 16 can be represented by:

$$p^{r}(T) = \int_{\Gamma} [V(Q)\,T^{i}(T,Q) + p^{r}(Q)\,U^{r}(T,Q) - p^{i}(Q)\,U^{i}(T,Q)]\,ds \qquad (17)$$

$$p^{i}(T) = \int_{\Gamma} [-V(Q)\,T^{r}(T,Q) + p^{r}(Q)\,U^{i}(T,Q) - p^{i}(Q)\,U^{r}(T,Q)]\,ds \qquad (18)$$

Discretization of the integral equations for surface pressure

For a numerical solution of Eqs 17 and 18, the boundary line is discretized into N subintervals respectively on both sides of Y-axis, as shown in Fig. 2. The above two equations can be then represented as the summation of the integral equations in each subinterval:

$$p^{r}_{m} = \sum_{j=1}^{N} \int_{S_j} \left[V_j T^{i}_{mj} + p^{r}_{j}\,U^{r}_{mj} - p^{i}_{j}\,U^{i}_{mj} \right] ds \qquad (19)$$

$$p^{i}_{m} = \sum_{j=1}^{N} \int_{S_j} \left[-V_j T^{r}_{mj} + p^{r}_{j}\,U^{i}_{mj} - p^{i}_{j}\,U^{r}_{mj} \right] ds \qquad (20)$$

When the subintervals are small enough, the velocity and the pressure over each subinterval can be treated as constants, i.e., V_j, p^{r}_{j} and p^{i}_{j} are constant. Based on this assumption, V_j, p^{r}_{j}, and p^{i}_{j} can be taken outside the integral, Eqs 19 and 20 then become:

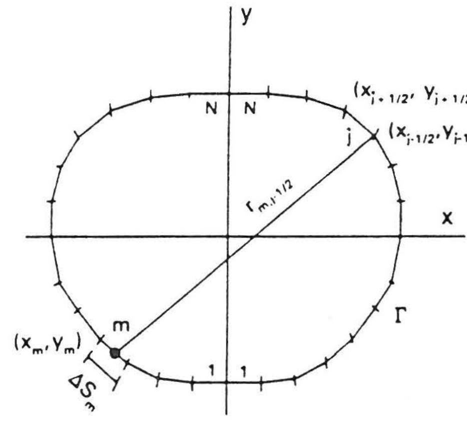

Fig. 2. General geometric consideration for an apple in a symmetric shape.

$$p^r_m = \sum_{j=1}^{N} \left[V_j I^i_{mj} + p^r_j L^r_{mj} - p^i_j L^i_{mj} \right] \quad (21)$$

$$p^i_m = \sum_{j=1}^{N} \left[V_j I^r_{mj} + p^r_j L^i_{mj} + p^i_j L^r_{mj} \right] \quad (22)$$

where I^i_{mj}, I^r_{mj}, L^i_{mj}, and L^i_{mj} are the integrals in the j^{th} subinterval given in the appendix, and their solutions can be obtained with numerical calculation on a HP9000/ 720 workstation by using some NAG subroutines [5]. The pressure for all the subintervals can be expressed simultaneously in a matrix form as follows:

$$\{p^r\} = [I^i_{mj}]\{V\} + [L^r_{mj}]\{p^r\} - - [L^i_{mj}]\{p^i\} \quad (23)$$

$$\{p^i\} = - [I^r_{mj}]\{V\} + [L^i_{mj}]\{p^r\} - - [L^r_{mj}]\{p^i\} \quad (24)$$

where $\{p^r\}$, $\{p^i\}$ and $\{V\}$ are mx1 matrices, $[I_{mj}r]$, $[I_{mj}i]$, $[L_{mj}r]$, and $[L_{mj}i]$ are NxN symmetric matrices, given in the appendix. Solving Eqs 23 and 24 yields the simplified equations for the surface pressure:

$$\{p^r\} = 2\{[1]-[L^r_{mj}]\}\{[I^r_{mj}]+[L^i_{mj}] \{[1]-[L^r_{mj}]\}^{-1}[I^r_{mj}]\{V\} = [E^r]\{V\} \quad (25)$$

$$\{p^i\} = 2\{[1]-[L^r_{mj}]\}\{[I^r_{mj}]+[L^i_{mj}] \{[1]-[L^r_{mj}]\}^{-1}[I^i_{mj}]\{V\} = [E^i]\{V\} \quad (26)$$

where [1] is called an unity matrix. Once the matrices $[I^r_{mj}]$, $[I^i_{mj}]$, $[L^r_{mj}]$, and $[L^i_{mj}]$ are determined, the surface pressure can then be derived. It can be seen that the matrices $[E^r]$ and $[E^i]$ depend only on the apple parameters such as the density, the Lamé constants, the resonant frequency, the shape, etc. When the matrices $[E^r]$ and $[E^i]$ are calculated for an apple, the surface pressure of the apple under different vibrational intensity can be derived from Eqs 25 and 26 simply by changing $\{V\}$. This can largely reduce the calculation work.

Acoustic pressure at any point in the external field

Once the surface pressure is determined, the acoustic pressure at any point in the external field can be calculated from Eq. 11. This equation can be transformed using the same approach as above to a numerical form similar to Eqs 21 and 22:

$$p^r_e = \sum_{j=1}^{N} \left[V_j I^i_{ej} + p^r_j L^r_{ej} - p^i_j L^i_{ej} \right] \quad (27)$$

$$p^i_e = \sum_{j=1}^{N} \left[-V_j I^r_{ej} + p^r_j L^i_{ej} - p^i_j L^r_{ej} \right] \quad (28)$$

where p_e denotes the pressure at an external point, p_j the pressure on the apple surface. In calculating P_e, the air properties such as the density of 1.291 kg/m^3, and the velocity of sound of 343 m/s are used to replace the properties of the apple in the calculation of each element of $[I_{mj}r]$, $[I_{mj}i]$, $[L_{mj}r]$, and $[L_{mj}i]$ as well as $\{V\}$.

RESULTS AND DISCUSSION

As an example, the surface of an apple is discretized into 14 sections with the mark numbers 1 and 14 corresponding to the two ends of the apple, and 8 to the apple equator, as shown in Fig. 3. By the finite element analysis, normal distribution of the velocity for the spherical mode is available [4]. As the velocity distribution becomes known, the surface pressure in each section as well as the pressure at any external field point can be then derived from the above numerical approaches.

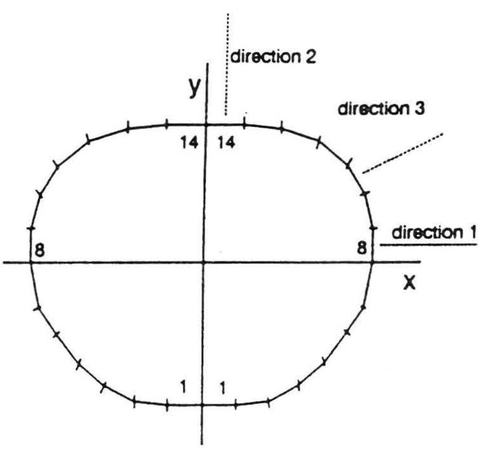

Fig. 3. An example of the geometry for studying the acoustic response of the apple.

Acoustic pressure

Figure 4 illustrates the distribution of the real part of the surface velocity as well as the real and imaginary parts of the pressure at the surface. The imaginary part of the velocity is zero. It is noted for the velocity and the pressure that the distribution of their real part is similar especially at the two ends of the apple. The fact that the vibration velocity at two ends is almost two times higher than that in the equator determines that the acoustic pressure at these ends is also much higher than at other parts on the apple surface. The acoustic vibration signal is much stronger at the two ends. For the acoustic pressure measurement using a

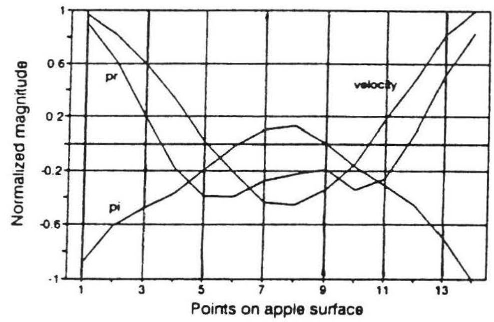

Fig. 4. Distribution of the real part of the velocity and the real and imaginary parts of the pressure on the apple surface.

microphone, it is easier to detect the vibration signal at these two ends of an apple.

The velocity curve shows one nodal line in section 5 and another nodal line in section 10. Along the surface between the sections 5 and 10, the highest velocity is found for section 8, the apple equator. It was also noted that there is no section where the magnitude of the surface pressure is zero. In section 5 and 10 the surface pressure is even higher than that in section 7 to 9 although this difference is relatively smaller compared with the velocity difference in these sections. It is obvious that the vibration of the spherical mode can probably be detected anywhere on the apple surface when the microphone is used as a sensor.

In the finite element simulation, the apple is assumed to be an elastic body, for which the imaginary part of the surface velocity is calculated to be zero. This means that during the vibration the velocity of different parts on the apple surface reaches its maximum amplitude or its zero simultaneously. However, for the sound pressure during the vibration, the existence of the imaginary part of the pressure indicates that there exist phase differences in pressure at different parts on the apple surface. When the pressure in one part reaches its maximum amplitude, the pressure in other parts does not, causing time delays. The delayed phase can be calculated according to both the real and the imaginary part of the pressure.

The pressure radiation in the air along the direction normal to the apple surface is illustrated in Fig. 5, where direction 1 corresponds to the apple equator (Fig. 3), direction 2 the apple shoulder, and direction 3 the nodal line area. A normalized pressure is a pressure divided by the maximum pressure, therefore is dimensionless. The pressure at distance of zero denotes the surface pressure. It is obvious that the pressure declines during the transmission in the air, and tends to become zero with the increasing distance away from the apple surface. Furthermore this decline is much sharper in the near field, within one or two centimetres from the apple surface, than in the far field. Therefore, in order to detect the vibration signal in a non-contact way, a microphone should be set as close as possible to the apple surface. Figure 5a also shows the different decline ratio in the air for the different positions. The pressure transmitted along the nodal line direction (direction 3) decreases faster than along the equator direction (direction 1). Although the surface pressure in the nodal line is higher than that in the equator, after merely 0.5 centimetre of transmission it becomes lower than the pressure transmitted for the same distance along the equator direction.

It can be concluded that some difference in the magnitude and phase for the vibration signal can be obtained when a microphone is used to replace an accelerometer. Concerning the interest of measuring the resonant frequency, this difference is of less importance.

Influence of apple firmness and density

The finite element simulation shows that the difference in the apple firmness and density does not change the velocity distribution of a mode, but may change the magnitude of its velocity [4]. These results were used in the Helmholtz integral simulation for the acoustic pressure.

Figure 5b illustrates the pressure radiation from section 8 when apples with different Young's modulus are subjected to a sinusoidal force of the same magnitude at their resonant frequencies. It is seen that the softer apple corresponds to a higher pressure radiation. It is also observed that the variation of the Young's modulus from 4.5 MPa to 4 MPa causes more change in the magnitude of the pressure than the variation from 4 MPa to 3.5 MPa. It thereby reveals that the pressure radiation for the harder apple is more sensitive to the variation of the apple firmness.

Figure 5c shows the influence of the apple density on the pressure radiation. The apple with a higher density corresponds to the higher pressure radiation. It is also noted that the variation of the density from 800 kg/m^3 to 860 kg/m^3 causes much less changes in the pressure than from 860 kg/m^3 to 920 kg/m^3. The pressure radiation for the apple with the higher density is more sensitive to the variation of the apple density.

The above observation can also be explained by the fact that the apple with a lower firmness or a higher density tends to have a lower resonant frequency, and therefore tends to vibrate with a bigger amplitude and a higher pressure radiation under the same excitation force. In such case to detect the acoustic pressure, a microphone can be set further away from the apple surface. Alternatively for such kind of apples, less excitation force is required when the microphone is set in a fixed distance away from the apple.

Influence of apple shape

Figure 6 shows the surface pressure and the pressure radiation in the air for two apples with different overall shape designated by the ratio of H/D with H the apple height and D the apple diameter. It seems that the H/D ratio does not influence considerably the pressure distribution on the apple surface especially at two ends of the apple, but may change the magnitude of the

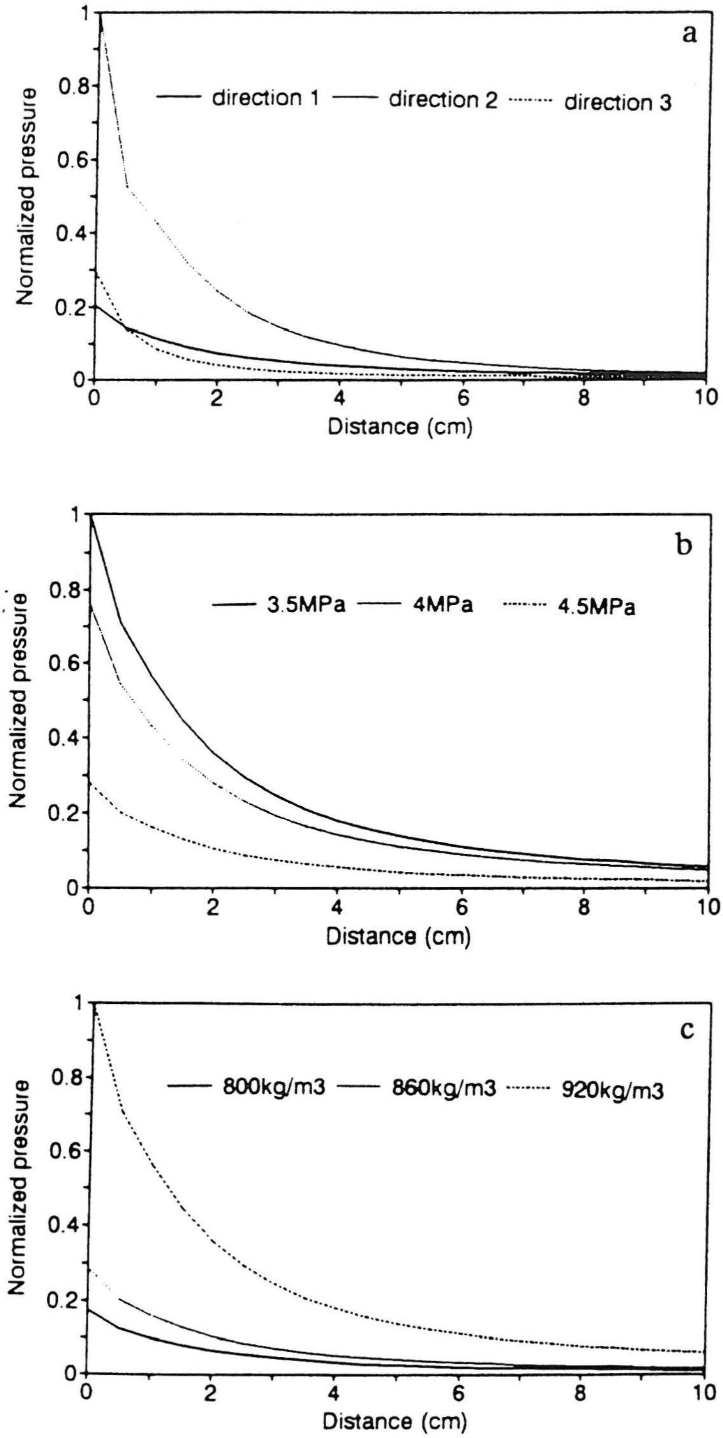

Fig. 5. Pressure radiation as a function of distance from the apple in the three directions shown in Fig. 3. (a), in direction 1 for different values of the apple firmness (b), and in direction 1 for different values of the apple density (c).

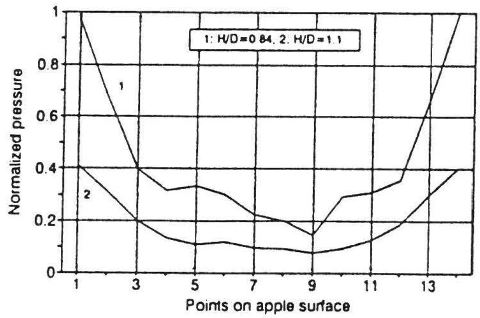

Fig. 6. Influence of the height to diameter ratio H/D of the apple on the pressure distribution along the apple surface.

pressure. The apple with a smaller value of H/D, or a flatter shape, tends to have a higher pressure radiation from the apple surface.

Influence of the transmission medium

Figure 7 shows the influence of the transmission medium on the pressure radiation in the external field, provided the same surface pressure. The medium with a lower density and a higher velocity of sound has less ability to transmit the pressure since the pressure declines more during the transmission. However in comparison with other factors such as the firmness, the density as well as the shape of the apple, the influence of the medium is relatively small.

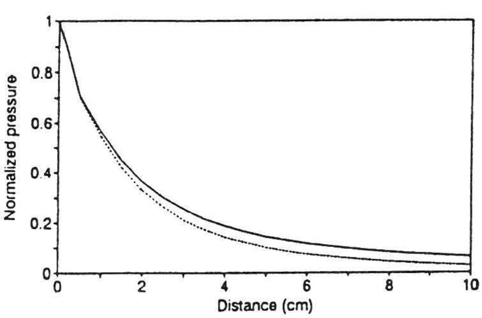

Fig. 7. Influence of the external transmission medium on the pressure radiation decline as a function of distance.

CONCLUSIONS

The surface pressure and the pressure at any external field point of a vibrating apple are given in the form of Helmholtz integrals along with a boundary condition. Considering the apple shape as a Y-axisymmetric revolution, the three dimensional acoustic problem for the spherical mode of the apple can first be simplified to the two dimensional acoustic problem. This is then solved by discretizing the boundary line into many subintervals, and performing numerical calculations for each interval.

The distribution of the surface pressure and the pressure radiation in the air from the equator, the shoulder and the nodal line are obtained for the spherical mode. The difference in the distribution between the surface pressure and the surface velocity indicates that the magnitude and the phase measured by a microphone can be a little different from that by an accelerometer. The fact that the acoustic pressure declines sharply while being transmitted in the external field suggests that the microphone should be set as close as possible to the apple in order to detect the response signal. A variation in the apple properties including the firmness, the density and the shape does not cause obvious changes in the distribution of the surface pressure, but may cause changes in its magnitude. The property of the air for the external field does not influence considerably the pressure decline during transmission.

It should be indicated that the solution is only concerned with a single spherical mode under sinusoidal vibration at its resonant frequency. A real apple shows many spherical modes in a narrow frequency band, and they may vibrate simultaneously. In this case the surface pressure is the sum of the pressure radiation caused by each mode at its resonant frequency. For this solution, full knowledge of the velocity distribution of each mode is required. Further research remains to be done.

ACKNOWLEDGEMENT

Financial support for this work came from the K.U.Leuven research fund and from the EEC through EUROFRU and CAMAR project No. 8001-CT91-0206.

REFERENCES

1. **Armstrong P., Zapp H.R., Brown G.K.**: Impulsive excitation of acoustic vibrations in apples for firmness determination. Trans. ASAE, 33(4), 1353-1359, 1990.
2. **Bell W.A., Meyer M.L., Zinn B.J.**: Predicting the acoustics of arbitrarily shaped bodies using an integral approach. AIAA J., 15, 813-820, 1977.
3. **Chen H., De Baerdemaeker J., Vervaeke F.**: Acoustic impulsive resonance of apples for monitoring texture change after harvest. Proc. Int. Conf. Agric. Eng., Beijing, China. International Academic Publishers, ISBN:7-80003-3/S125, 1, IV, 30-38, 1992.
4. **Chen H.**: Unpublished data. 1992.
5. **Chen H.**: Analysis on the acoustic impulse resonance of apples for nondestructive estimation of fruit quality. Ph.D. Thesis, Department of Agricultural Engineering, Katholieke Universiteit Leuven, Belgium, 1993.
6. **Chertock G.**: Sound radiation from vibrating surface. J. Acoustical Soc. Am., 36(7), 1305-1313, 1964.
7. **Cooke, J.R., Rand R.H.**: A mathematical study of resonance in intact fruits and vegetables using a 3-media elastic sphere model. J. Agric. Eng. Res., 18, 141-157, 1973.
8. **Copley L.G.**: Integral equation method for radiation from vibrating bodies. J. Acoustical Soc. Am., 41, 807-816, 1966.
9. **Finney E.E., Jr., Norris K.H.**: Instrumentation for investigating dynamic mechanical properties of fruits and vegetables. Trans. ASAE, 11(1), 94-97, 1968.
10. **Finney E.E., Jr.**: Random vibration techniques for nondestructive evaluation of peach firmness. J. Agric. Eng. Res., 16(1), 81-87, 1971.
11. **Olson H.F.**: Elements of Acoustical Engineering (2nd edition). D. Van Nortrand Company, Inc., 1947.
12. **Huarng L.D., Chen P., Upadhyaya S.K.**: Determination of acoustic vibration modes in apples. ASAE Paper No. 92-6510, 1992.
13. **Latcha M.A., Akay A.**: Application of the Helmholtz integral in acoustics. J. Vibration, Acoustics, Stress, and Reliability in Design, Trans. SAMA, 108, 447-453, 1986.
14. **Van Woensel G., Verdonck E., Snoeys R., De Baerdemaeker J.**: Measuring the mechanical properties of apple tissue using modal analysis. The 2nd Int. Modal Analysis Conf., Leuven, Belgium, 1984.
15. **Yamamoto H., Iwamoto M., Haginuma S.**: Acoustic impulse response method for measuring natural frequency of intact fruits and preliminary applications to internal quality evaluation of apples and watermelons. J. Texture Study, 11, 117-136, 1980.

APPENDIX

$$V(Q) = \rho\omega v(Q)x$$

$$T(T,Q) = \frac{1}{2\pi} * \int_{-\pi}^{\pi} \frac{e^{ikr}}{r} \, d\theta = T(Q,T)$$

$$U(T,Q) = \frac{1}{2\pi} * \int_{-\pi}^{\pi} \frac{\partial}{\partial n} \frac{e^{ikr}}{r} \, d\theta = U(Q,T)$$

$$I^{i}_{mj} = * \int_{s_j} T^{i}_{mj} \, ds = I^{i}_{jm}$$

$$I^{r}_{mj} = * \int_{s_j} T^{r}_{mj} \, ds = I^{r}_{jm}$$

$$L^{i}_{mj} = * \int_{s_j} U^{i}_{mj} \, ds = L^{i}_{jm}$$

$$L^{r}_{mj} = * \int_{s_j} U^{r}_{mj} \, ds = L^{r}_{jm}$$

Continued

$$\{p^r\} = \begin{pmatrix} p_1^r \\ p_2^r \\ \cdot \\ \cdot \\ \cdot \\ \cdot \\ p_N^r \end{pmatrix}, \quad \{p^i\} = \begin{pmatrix} p_1^i \\ p_2^i \\ \cdot \\ \cdot \\ \cdot \\ \cdot \\ p_N^i \end{pmatrix}, \quad \text{and} \quad \{V\} = \begin{pmatrix} V_1 \\ V_2 \\ \cdot \\ \cdot \\ \cdot \\ \cdot \\ V_N \end{pmatrix}$$

$$\left[I^r_{mj}\right] = \begin{pmatrix} I^r_{11} & I^r_{12} & \cdot & \cdot & I^r_{1N} \\ & I^r_{22} & & & \cdot \\ & & \cdot & & \cdot \\ & & & \cdot & \cdot \\ & & & & I^r_{NN} \end{pmatrix} \quad \left[I^i_{mj}\right] = \begin{pmatrix} I^i_{11} & I^i_{12} & \cdot & \cdot & I^i_{1N} \\ & I^i_{22} & & & \cdot \\ & & \cdot & & \cdot \\ & & & \cdot & \cdot \\ & & & & I^i_{NN} \end{pmatrix}$$

$$\left[L^r_{mj}\right] = \begin{pmatrix} L^r_{11} & L^r_{12} & \cdot & \cdot & L^r_{1N} \\ & L^r_{22} & & & \cdot \\ & & \cdot & & \cdot \\ & & & \cdot & \cdot \\ & & & & L^r_{NN} \end{pmatrix} \quad \left[L^i_{mj}\right] = \begin{pmatrix} L^i_{11} & L^i_{12} & \cdot & \cdot & L^i_{1N} \\ & L^i_{22} & & & \cdot \\ & & \cdot & & \cdot \\ & & & \cdot & \cdot \\ & & & & L^i_{NN} \end{pmatrix}$$